Amino Acids (2010) 39:1147–1160
DOI 10.1007/s00726-010-0549-8

ORIGINAL ARTICLE

Structural elucidation of Leuprolide and its analogues in solution: insight into their bioactive conformation

Despina K. Laimou · Maria Katsara · Minos-Timotheos I. Matsoukas · Vasso Apostolopoulos · Anastassios N. Troganis · Theodore V. Tselios

Received: 29 October 2009 / Accepted: 25 February 2010 / Published online: 31 March 2010

Abstract Leuprolide [DLeu^6, NHEt^{10}]GnRH, a potent gonadotropin-releasing hormone (GnRH) agonist, is used in a wide variety of hormone-related diseases like cancer and endometriosis. In this report, the conformational behaviour of Leuprolide and its linear synthetic analogues, namely [Tyr^5(OMe), DLeu^6, Aze^9, NHEt^{10}]GnRH **(1)** and [Tyr^5(OMe), DLeu^6, NHEt^{10}]GnRH **(2)** have been studied in DMSO and H_2O solutions by means of 2D nuclear magnetic resonance (NMR) experiments and detailed molecular dynamics (MD) simulations. The aim was to identify the conformational requirements of GnRH analogues for agonistic activity. This approach is of value as no crystallographic data are available for the GnRH receptor (G protein-coupled receptor, GPCR). The NOE data indicate the existence of a β-turn type I in the 2–5 segments of Leuprolide and its linear analogues in the case of using DMSO-d_6 as solvent, whereas a β-turn type II in the 3–6 segments is indicated using D_2O as solvent. The final structures fulfil the conformational requirements that are known, in the literature, to play a significant role in receptor recognition and activation. Finally, the linear analogues **(1)** and **(2)** are biologically active when tested against the human breast cancer cell line, MCF-7.

Keywords Gonadotropin-releasing hormone (GnRH) · Leuprolide · Nuclear magnetic resonance · Bioactive conformation · Molecular dynamics

Abbreviations

GnRH	Gonadotropin releasing hormone
NMR	Nuclear magnetic resonance
MD	Molecular dynamics

Introduction

Gonadotropin-releasing hormone (GnRH), plays a significant role in the reproductive system. GnRH is induced in the hypothalamus regulating and releasing the gonadotropins, luteinizing (LH) and follicle-stimulating (FSH) hormones, which modulate the secretion of steroid hormones. On the other hand, the production of gonadotropins could be decreased by down regulation of GnRH receptors (Conn and Crowley 1991; Hazum and Conn 1988). Many diseases, such as prostate and breast cancer, endometriosis and uterine leiomyomas, are stimulated by steroid hormones. GnRH analogues, triptorelin, leuprolide, buserelin, goserelin, nafarelin and histrelin, have important applications in the treatment of these sex hormone dependent diseases (Kaufmann et al. 1989; Scambia et al. 1988; Ayub and Levell 1990). Leuprolide ([DLeu^6, NHEt^{10}]GnRH), is a

Electronic supplementary material The online version of this article (doi:10.1007/s00726-010-0549-8) contains supplementary material, which is available to authorized users.

D. K. Laimou · M. Katsara · M.-T. I. Matsoukas · T. V. Tselios (✉)
Department of Chemistry, University of Patras, Patras 26500, Greece
e-mail: ttselios@upatras.gr

M. Katsara · V. Apostolopoulos
Immunology and Vaccine Laboratory, Burnet Institute (Austin Campus), Studley Road, Heidelberg, Victoria 3084, Australia

A. N. Troganis (✉)
Department of Biological Applications and Technologies, University of Ioannina, Ioannina 45110, Greece
e-mail: atrogani@cc.uoi.gr

synthetic altered peptide ligand (APL) of GnRH with agonistic activity that suppresses the secretion of LH and FSH, when administered by subcutaneous or intramuscular injection in long term, achieving castrate levels for testosterone in prostate cancer patients. Leuprolide is susceptible to the proteolytic enzymes due to its peptidic characteristic resulting in low intestinal absorption and bioavailability (less that 1%) following either oral or intraduodenal injections in several animal models. The GnRH analogues can be hydrolyzed at three bonds Trp^3-Ser^4, Ser^4-Tyr^5, Tyr^5-Gly^6, the first one being the preferred (Stephenson and Kenny 1988).

The de novo design and synthesis of peptide mimetics (stable non-peptide chemical moieties) is a central field of medicinal chemistry, that is instrumental to several areas of science and technology. A combination of advanced 2D-nuclear magnetic resonance (NMR) and molecular modelling techniques has proved to be the cornerstone in the rational drug design of non-peptide mimetics, considered to be the new and the next generation of drugs. NMR in combination with computational analysis is a reliable technique in order to provide information about the conformation and the stereoelectronic properties of a biological active peptide especially when no crystallographic data are available. This information could be used for the rational design of potent non-peptide mimetics using the most important for receptor activation pharmacophore groups placed on an appropriate rigid organic template.

Leuprolide is a good starting point for intensive conformational studies and rational drug design of non-peptide mimetics. Other research groups (Meyer et al. 2002) have studied the conformational characteristics of Leuprolide using NMR and circular dichroism under different solution conditions (TFE/water). Therefore, this work is focussed on the investigation of the putative bioactive structures of Leuprolide, [DLeu^6, NHEt^{10}]GnRH, and its two rationally designed altered peptide ligands (APLs) namely: [Tyr^5(OMe), DLeu^6, Aze^9, NHEt^{10}]GnRH **(1)**, [Tyr^5(OMe), DLeu^6, NHEt^{10}]GnRH **(2)** using 2D NMR and molecular dynamics techniques. The NMR studies are accomplished using DMSO and H_2O solutions in order to emulate the GnRH receptors' environment and to compare the obtained conformations in a polar (H_2O, dielectric constant 80.1 at 25°C) and in an aprotic-lipophilic solvent (DMSO, dielectric constant 46.7 at 25°C). Non-natural amino acids have been extensively used in several peptide analogues in order to restrict the conformational flexibility, to enhance the stability in enzymatic degradation and finally to improve bioavailability and pharmacokinetic. In this study, the non-natural amino acid azetidine (Aze, four member ring) at position 9 was used in order to improve the ability of the synthesised analogue to bind to its receptor and to stabilise better the conformational integrity of the peptide. Moreover, substitution of Tyr^5 with Tyr(OMe) aimed at avoiding the desensitisation of GnRH receptors (Keramida et al. 1996; Matsoukas et al. 1997). It was reported that the [Tyr^5(OMe)] GnRH analogue exerted a lower degree of receptor desensitisation than GnRH in terms of pituitary GnRH receptor (Keramida et al. 1996). Finally, as it is reported in the literature, the introduction of DLeu (Leuprolide) at position 6 intended to stabilise a U shape conformation of GnRH improving the binding affinity (Momany 1976, 1978; Söderhäll et al. 2005). The amino acid sequences of synthesised linear analogues in comparison to mammalian GnRH and Leuprolide are shown in Table 1.

The putative bioactive conformation of Leuprolide and its synthetic APLs are an essential tool in the understanding of physicochemical properties for the agonistic biological activity. Within this scope, this study firstly was focussed on the conformational analysis of Leuprolide, which despite its widespread use only limited information based on spectroscopic evidence regarding the solution conformation can be found in the literature (Meyer et al. 2002). On the other hand, no crystallographic data are available due to the nature of the GnRH receptor (GPCR type). Moreover, the homology modelling of GnRH receptor using the rhodopsin X-ray structure does not give reliable conformations (low degree of alignment) which indicate the drug design based on the receptor-ligand interaction difficult to be achieved. Consequently, detailed pharmacophore analysis of Leuprolide and its linear analogues using NMR and Molecular Dynamics will be a useful approach for the rational drug design based on ligand. For this reason, experimental 1D and 2D NMR spectroscopic methods and molecular dynamics (MD) simulations have been applied to establish a representative conformation of Leuprolide and its linear analogues in DMSO and H_2O solutions. The aim was not only to calculate the average structure that complies with all NOEs and represent the real situation in solution, but also, to shed light into the whole conformational ensemble. Such approach reveals many energetically favoured conformations and agrees with the general accepted concept that peptides bind to their receptor in a low energy conformation, not necessarily the global minimum. The proposed conformations for each analogue are indeed low energy structures, in which a range of the experimental NOE distance restraints is in accordance with the conformation obtained by the molecular simulation. This work establishes the evidence that using both experimental NOE data and theoretical modelling studies could help to explore and understand the stereoelectronic requirements for GnRH typed drugs in order to design non-peptide

Table 1 Primary structure of the synthesised linear GnRH analogues, mammalian GnRH and Leuprolide

Name	Amino acid sequence									
	1	2	3	4	5	6	7	8	9	10
Mammalian GnRH	pGlu	His	Trp	Ser	Tyr	Gly	Leu	Arg	Pro	$GlyNH_2$
Leuprolide, [DLeu^6, NHEt^{10}] GnRH	–	–	–	–	–	D-Leu	–	–	–	NHEt
[Tyr^5(OMe), DLeu^6, Aze^9, NHEt^{10}] GnRH (1)	–	–	–	–	Tyr(OMe)	D-Leu	–	–	Aze	NHEt
[Tyr^5(OMe), DLeu^6, NHEt^{10}] GnRH (2)	–	–	–	–	Tyr(OMe)	D-Leu	–	–	–	NHEt

"mimetic" of GnRH, analogues with increased stability to enzymatic degradation.

Materials and methods

Synthetic procedure

Acetate salt of Leuprolide was obtained from Bachem Chemical Company with product code H-4060, [DLeu^6, NHEt^{10}]GnRH. 2-chlorotrityl chloride resin (0.7–1.0 mmol Cl^-/g resin, 200–400 mesh), Fmoc-Arg(Pbf)-OH, Fmoc-Leu-OH, Fmoc-DLeu-OH, Fmoc-Ser(tBu)-OH, Fmoc-Trp-OH, Fmoc-His(Trt)-OH, pGlu-OH and Fmoc-Pro-OH were obtained from Chemical and Biopharmaceutical Laboratories of Patras, Patras, Greece. All solvents and other reagents were purchased from Merck, Sigma-Aldrich and Fluka companies. DC-Alufolien Kieselgel 60 (Merck) was used for thin layer chromatography (TLC) analysis of synthetic products with the following eluant solvent: *n*-butanol/acetic acid/water (BAW) 4:1:1 (v/v/v). Peptides were purified by semi-preparative reverse phase high performance liquid chromatography (RP-HPLC) with a Waters system equipped with a 600E controller and a Waters 996 photodiode array UV detector. The analysis was controlled by an operating Millenium 2.1system and a Nucleosil C-18 reversed phase column (250 × 10 mm with 7 μm packing material). Electron spray ionisation mass spectroscopy (ESI–MS) experiments were performed with a TSQ 7000 spectrometer (Electrospray Platform LC of Micromass) coupled to a MassLynx NT 2.3 data system.

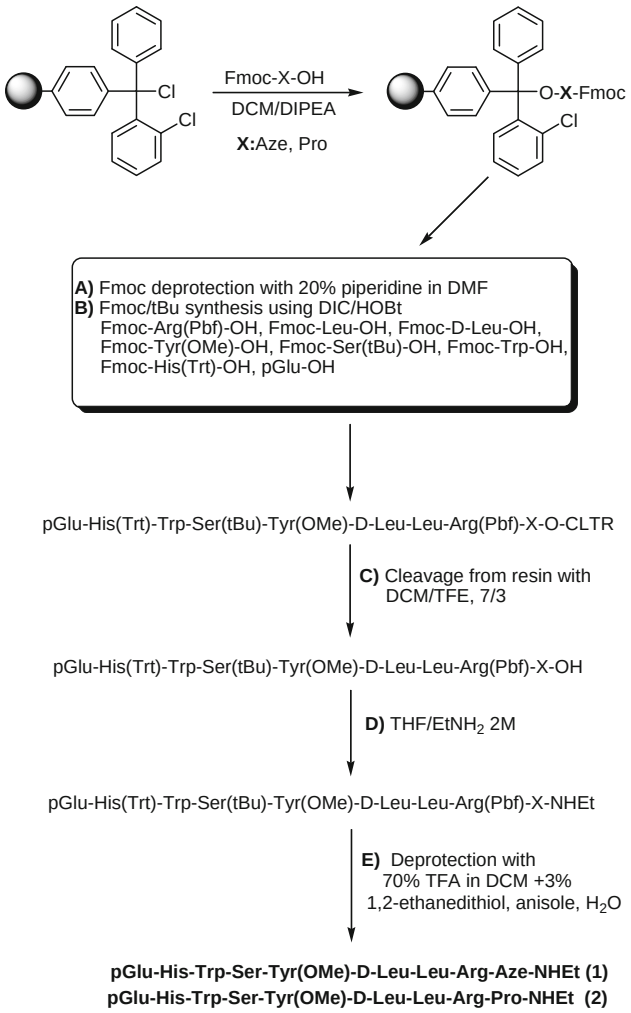

Scheme 1 Synthetic procedure for linear analogues [Tyr^5(OMe), DLeu^6, Aze^9, NHEt^{10}]GnRH and [Tyr^5(OMe), DLeu^6, NHEt^{10}]GnRH

Synthesis of linear analogues 1 and 2

The linear peptides were prepared on CLTR-Cl (1 g for each peptide) using the Fmoc/tBu, methodology (Scheme 1). The first N^{α}-Fmoc (9-fluorenylmethyloxycarbonyl)-protected amino acid, Fmoc-Aze-OH (1 equiv) for analogue **(1)** and Fmoc-Pro-OH (1 equiv) for analogue **(2)**, was coupled (esterified) to the resin in the presence of diisopropylethylamine (DIPEA) (4.5 equiv, 0.75 mL) in dichloromethane (DCM) in 1 h at RT. A mixture of DCM/MeOH/DIPEA (85:10:5, 7 mL) was then added and the mixture was stirred for another 10 min at RT. The Fmoc-Aze-resin and Fmoc-Pro-resin were subsequently filtered and washed with DCM (3 × 10 mL), 2-propanol (iPrOH) (2 × 10 mL) and *n*-hexane (2 × 10 mL) and dried under vacuum for 24 h.

The remaining protected peptide chains were assembled by sequential couplings of the appropriate amino acids (2.5 equiv) in the presence of *N*,*N*′-diisopropylcarbodiimide (DIC) (2.75 equiv) and 1-hydroxybenzotriazole (HOBt)

(3.75 equiv) in *N*,*N*-dimethylformamide (DMF) for 4–6 h (Tselios et al. 2000a, b; Matsoukas et al. 2005; Keramida et al. 2006). The following Fmoc protected amino acids were used for the synthesis: Fmoc-Arg(Pbf)-OH, Fmoc-Leu-OH, Fmoc-DLeu-OH, Fmoc-Tyr(OMe)-OH, Fmoc-Ser(tBu)-OH, Fmoc-Trp-OH, Fmoc-His(Trt)-OH and pGlu-OH (Scheme 1). The completeness of each coupling was verified by the Kaiser test and TLC using a BAW, 4:1:1 (v/v/v) eluent system and the Fmoc protecting group was removed by treatment with piperidine solution (20% in DMF, 2 × 20 min). The synthesised protected peptides on the resin were dried under vacuum (1.44 and 1.40 g, respectively) and then cleaved with the splitting solution DCM/TFE (7:3) for 2 h at RT. The mixtures were filtered, the solvents were removed on a rotary evaporator and the obtained oily products were precipitated from cold dry diethyl ether as amorphous white solids (0.36 and 0.34 g, respectively). The conversion of the above peptides to ethylamide was achieved using a solution of THF/$EtNH_2$ 2 M (4 equiv) with the presence of (1.75 equiv) and DIC (1.5 equiv). After stirring for 12 h at RT, the solvents were removed on a rotary evaporator and the obtained oily products were precipitated from water as amorphous white solids (0.32 and 0.30 g, respectively). The dried linear protected peptides were treated with 70% TFA in DCM in the presence of 0.3% 1,2-ethanedithiol, anisole and H_2O as scavengers for 5 h at room temperature. The solvents were removed on a rotary evaporator and the obtained oily products were precipitated from cold dry diethyl ether as amorphous light-yellow solids (0.18 and 0.13 g, respectively). The crude peptide products were further purified by semi-preparative RP-HPLC (column: Nucleosil C18, 5 μm, 4.6 × 250 mm), eluents: A, 0.08% TFA/H_2O, B, 0.08% TFA/CH_3CN, gradual gradient: from 20 to 100% B in 27 min, flow rate: 3 mL/min, detection 214 nm, 254 nm t_R: 13.4 min (1); 13.8 min (2) and were identified by ESI–MS: M = 1209.64, M + 2H/2 = 605.53 (1); M = 1223.42, M + 2H/2 = 612.7 (2).

The conversion of final purified compounds from TFA to acetate salt was achieved using a cation-exchange chromatography with column of (carboxylmethyl)cellulose (Whatman CM23) and following the protocol previously described (Matsoukas et al. 2005).

Nuclear magnetic resonance spectroscopy

The NMR spectra were recorded on a Bruker AVANCE 400 MHz spectrometer at 298 K, using DMSO-d_6 as solvent and at 278 K using H_2O–D_2O 90–10 as solvent. The concentration of the samples was 5 mg/ml, approximately. Routine parameters were used recording the ^1H spectra. The sweep width was 6,000 Hz and the chemical shifts are reported with respect to the resonance of the solvent in DMSO-d_6 solutions, while in H_2O–D_2O solutions the chemical shifts are reported with respect to the resonance of TSP, which was used as internal standard. All 2D spectra were acquired using TPPI method for quadrature detection. The 2D measurements were recorded using 512 increments of 2 K complex data points and 80 scans per increment for 2D ^1H NOESY and 16 scans for 2D ^1H TOCSY experiments, respectively. The mixing time for NOESY spectra was 350 ms, and that for TOCSY was 90 ms. In H_2O–D_2O solutions, the WATERGATE-5 pulse sequence was used for the suppression of the signal of the water. Data were processed using the TopSpin standard software. The t_1 dimension was zero-filled to 1 K real data points, and 60° phase-shifted square sine bell window functions were applied in both dimensions.

Theoretical calculations

Molecular modelling

The computer calculations were performed on a Pentium IV 2.14 GHz workstation using Discovery Studio v2.0 2005 by Accelrys Software Inc. Molecular dynamics simulations were performed and the derived conformations were examined for consistency with experimental distance and dihedral information derived from the obtained NOEs. Thus, populations of various conformers that represent local minima at the potential energy surface were identified.

Generating the starting conformation

The starting conformations of Leuprolide [DLeu^6, NHEt^{10}]GnRH and its two linear analogues: [Tyr(OMe)^5, DLeu^6, Aze^9, NHEt^{10}]GnRH (1) and [Tyr(OMe)^5, DLeu^6, NHEt^{10}]GnRH (2) were extendedly built, consisting of L- and D-amino acids, using the CHARMm force field (Brooks et al. 1983). The studies were performed using two different solvents DMSO (dielectric constant 47) (Chen et al. 2006; Mantzourani et al. 2006, 2007, 2008) and H_2O (dielectric constant 80) in agreement with the NMR experiments. Solvent model generalized born with a simple switching (GBSW) (Ryckaert et al. 1977) was used, as well as the SHAKE algorithm which serves satisfying bond geometry constraints during the molecular dynamics simulations. The structures were then minimised using a succession of three methods: steepest descents (SD) algorithm to remove unfavourable steric contacts, then conjugate gradient (CONJ) to find its local minimum, followed by truncated Newton (TN). TN is the most efficient large scale non-linear optimisation algorithm known. In all cases, energy convergence criterion is the root mean square deviation (RMSD) force $\leq$ 0.001 kcal mol^{-1}Å^{-1}.

Molecular dynamics studies

Two sets, one completely unrestrained and one restrained using NOE constraints (distances and dihedrals), of MD runs were performed using the CHARMm force field as follows: heating, from 0 to 300 K gradually and equilibration were set with a time step of 0.002 ps for a total time of 0.1 ns while the time step of production was 0.002 ps for a total time of 1 ns. Parameters on saving results frequencies were set in such a way in order to extract 500 conformations for each molecule.

The first set of dynamics was completely unrestrained so that the analogues could obtain any energy permissible conformations due to their freedom. Moreover, a set of dihedral restrained dynamic trajectory was followed but the conformations were not decent enough with high energies due to the limited conformational freedom (data not shown).

Six conformations were selected according to the NMR results (dihedral angles, distances). Total energy was another criterion in order to select the final conformation for each analogue. The selected structures had backbone dihedral angles φ and ψ within the core region of the Ramachandran map (Ramachandran and Sasisekharan 1968; Ramakrishhan and Ramachandran 1965) and trans ω dihedral angles (Laskowski et al. 1993). Minimisation protocols were performed on the chosen structures using steepest descent (SD) and conjugate gradient (CG) algorithms, for 10,000 steps and RMSD 0.001 Å as energy convergence criterion.

Biological evaluation of synthesised analogues in MCF-7 cancer cell line

Cell culture and Dextran Charcoal stripped FCS (FCS/DCC)

The human breast adenocarcinoma cell line, MCF-7, was obtained from Burnet Institute (Austin Campus), VIC, Australia. The cells were maintained in Dulbecco's Modified Eagle's minimal essential Medium (DMEM; Gibco/BRL) without phenol red, supplied with 4 mM L-glutamine, 100 units/ml penicillin, 100 μg/ml streptomycin, 0.6 μg/ml insulin, 100 nM β-estradiol and 5% charcoal-stripped foetal calf serum FCS at 37°C in a humidified atmosphere of 8% CO_2 in air.

Estrogenic compounds were removed from serum by incubating 100 ml of foetal calf serum with 10 ml precipitated dextran coated charcoal (DCC). The dextran charcoal stripped solution was made by adding 5 g activated charcoal (Sigma) with 0.5 g dextran, Mr 200,000 (Sigma), in 2 ml 1.0 M Tris buffer, pH 7.4 and then brought to 200 ml with double distilled water. The mixture was incubated in 56°C for 30 min. The charcoal was removed by centrifugation at 3,000 rpm twice and was then filtered with 0.22 μm filter and stored at −20°C.

Cell proliferation assay [^{3}H] uptake

The cells were stripped of endogenous steroids by successive passages in DMEM without phenol red containing 10% then 5% charcoal-stripped foetal calf serum (FCS/DCC) (Vignon et al. 1987) 2×10^3 cells were seeded in 96-well round bottom plates with DMEM without phenol red media containing 5% charcoal-stripped FCS, without analogues. The following day the cells were treated with 1×10^{-7}– 1×10^{-10} M peptide analogues; Leuprolide, analogue **1** and **2**. The peptide analogues and media were replaced every two days and cultured in total for 6 days. On day 6, 1 μCi of [^{3}H]-thymidine was added to each well and incubated for 6 h. [^{3}H]thymidine uptake was measured by harvesting cells onto glass fibre filters and radioactive counts (cpm) were detected by a scintillation counter (β-counter). The percentage inhibition was calculated as: $[(cpm_{cells\ alone} - cpm_{analogue})/cpm_{cells\ alone}] \times 100\%$.

Results and discussion

NMR characterisation of [DLeu^6, NHEt^{10}]GnRH (Leuprolide), [Tyr(OMe)^5, DLeu^6, Aze^9, NHEt^{10}]GnRH (1) and [Tyr(OMe)^5, DLeu^6, NHEt^{10}]GnRH (2) in DMSO-d_6

Despite the presence of multiple conformations of small, especially linear, peptides in solution (due to their flexibility), NMR techniques have been widely used to determine the presence of conformers with distinguishable populations in linear or cyclic peptides, peptide fragments derived from protein sequences, peptides of de novo design, etc. (Morikis et al. 2002; Meyer et al. 2002; Mantzourani et al. 2008). Such studies typically require the use of two-dimensional correlation spectroscopy, usually TOCSY and NOESY experiments. In our studies, TOCSY and NOESY experiments were performed for resonance assignment of the protons, the identification of the amino acid sequencing and the establishment of the NOE connectivities. The results of the chemical shifts and the observed inter-residue cross-peaks in the NOESY spectrum and their intensities for [Tyr(OMe)^5, DLeu^6, Aze^9, NHEt^{10}]GnRH (1) are reported in Tables 2, and 3. The same results for [Tyr(OMe)^5, DLeu^6, NHEt^{10}]GnRH (2) and Leuprolide are included in the supplementary material (Tables S1–S4). The proton chemical shifts of Leuprolide and of two analogues are almost identical, indicating the similarity of their structures in solution.

Table 2 ^{1}H chemical shifts (ppm) of the residues in [Tyr(OMe)^{5}, DLeu^{6}, Aze^{9}, NHEt^{10}]GnRH (**1**) analogue at 298 K in DMSO-d_6 and in H_2O-D_2O 90-10 (*italics*)

	Residue	NH	αH	βH	Others
1	pGlu	7.67	3.97	1.71	γH:2.15;2.04
		7.83	*4.20*	*2.30*	*γH:1.63*
2	His	8.11	4.57	3.01;2.89	2H:8.72;4H:7.19
		8.51	*4.62*	*3.09;3.05*	*2H:8.35;4H:7.12*
3	Trp	8.06	4.62	3.13;2.95	2H:7.11;*7.19*, 4H:7.60;*7.56*
		8.32	*4.67*	*3.16*	5H:6.90;*7.11*, 6H:7.02;*7.23*
					7H:7.31;*7.49*, NH:10.80;*10.16*
4	Ser	8.28	4.35	3.59;3.51	
		8.25	*4.27*	*3.75;3.65*	
5	Tyr(OMe)	8.02	4.49	2.94;2.77	2,6H:7.14;*7.15* 3,5H:6.77;*6.91*
		8.01	*4.42*	*3.04;2.88*	CH_3:3.64;*3.70*
6	D-Leu	8.10	4.25	1.35	δH: 0.80;0.76
		8.29	*4.09*	*1.39*	*γH:1.39, δH: 0.77;0.67*
7	Leu	8.11	4.29	1.44;1.56	δH: 0.86;0.80
		8.27	*4.35*	*1.65*	*γH:1.55, δH:0.91;0.84*
8	Arg	8.11	4.17	1.69	γH:1.53, δH:3.09, NH:7.54
		8.42	*4.10*	*1.60;1.68*	*γH:1.48, δH:3.07, NH:7.15*
9	Aze		4.53	2.37;2.08	γH:4.19;4.10
			4.60	*2.47;2.18*	γH:4.12;4.09
10	NHEt	7.87	3.07	0.99	
		8.07	*3.20*	*1.07*	

According to theoretical studies which were accomplished using molecular modelling techniques, it is proposed that GnRH agonists are predicted to assume a U-shape upon binding to the receptor model. This U-shape form is supported by the existence of a type II' β-turn which is centred in residues 5–8 of the molecule (Söderhäll et al. 2005). Therefore, in this study, we examine the relevance of the observed NOEs with the expected NOEs for the common type of β-turn (type I and II). This can be achieved by examining specific H^N-H^N, H^α-H^N and H^β-H^N connectivities, according to Wuthrich (1986) and Morikis et al. (2002).

Examining the H^α/side chain (δ_1)-H^N (δ_2) region of the TOCSY spectrum (Fig. 1a) of the [Tyr(OMe)^5, DLeu^6, Aze^9, NHEt^{10}]GnRH (1), the spin system of all residues, with the exception of Aze^9, has been identified. The Aze residue could not be identified due to the lack of an H^N proton in its molecule. So, Aze residue has been identified from the well known pattern of γ–protons at 4.0–4.2 ppm approximately. Chemical shift overlaps in both the H^α and H^N of DLeu^6/Leu^7 is present. Also, chemical shift overlaps in the H^N of His^2/Leu^7/Arg^8 and to a lesser extent of Trp^3/DLeu^6 are present. Fsmallinally, chemical shift overlaps partially in the H^α of Ser^4/Leu^7 and His^2/Trp^3 are present. These overlaps are a strong indication of the flexibility of this analogue. Figure 1b shows the H^α (δ_1)-H^N (δ_2) region of the NOESY spectrum of analogue 1. Sequential connectivities corresponding to intra-residue H^α(i) - H^N(i) and short range H^α(i)-H^N(i + 1) NOE cross-peaks are observed in Fig. 1b, but only the intra-residue cross-peaks are labelled for simplicity. In addition, two weak H^α(i)-H^N(i + 2) cross-peaks corresponding to pGlu^1 H^α-Trp^3 H^N and to Trp^3 H^α-Tyr^5 H^N are observed (Fig. 1b), which are consistent with the presence of a β-turn. Figure 1c shows the H^N (δ_1)-H^N (δ_2) region of the NOESY spectrum of [Tyr(OMe)^5, DLeu^6, Aze^9, NHEt^{10}]GnRH (1), where the observed H^N(i)-H^N(i + 1) cross-peaks are labelled. Medium to strong intensity cross-peaks corresponding to Trp^3 H^N-Ser^4 H^N and Ser^4 H^N-Tyr^5 H^N NOEs are observed which are consistent with the presence of a type I β-turn in the segment His^2-Trp^3-Ser^4-Tyr^5. This is further confirmed by the existence of the medium intensity Trp^3 H^α-Ser^4 H^N cross-peak which is observed in Fig. 1b. Also, looking closer at the $H^\beta(\delta_1)$/$H^N(\delta_2)$ region of the spectrum, a very weak H^β(i)-H^N(i + 2) cross-peak is observed, corresponding to the Trp^3 H^β-Tyr^5 H^N NOE (Fig. 1d). The above NOE data is consistent with the presence of a but observable population of a type I β-turn in the segment His^2-Trp^3-Ser^4-Tyr^5 of [Tyr(OMe)^5, DLeu^6, Aze^9, NHEt^{10}]GnRH (1). Of course, it has to be mentioned, at this point, that a type III β-turn cannot be excluded. A type III β-turn has characteristic dihedral angles for the residue 2 and 3 (Trp^3 and Ser^4 in our case) of the turn (Φ_2, Ψ_2) = (−60°, −30°) and (Φ_3, Ψ_3) = (−60°, −30°) compared with the type I β-turn which has dihedral angles (Φ_2, Ψ_2) = (−60°, −30°) and (Φ_3, Ψ_3) = (−90°, 0°).

Table 3 Observed inter-residue cross-peaks in the NOESY spectrum and their intensities for [Tyr(OMe)^5, DLeu^6, Aze^9, NHEt^{10}]GnRH (**1**) analogue at 298 K

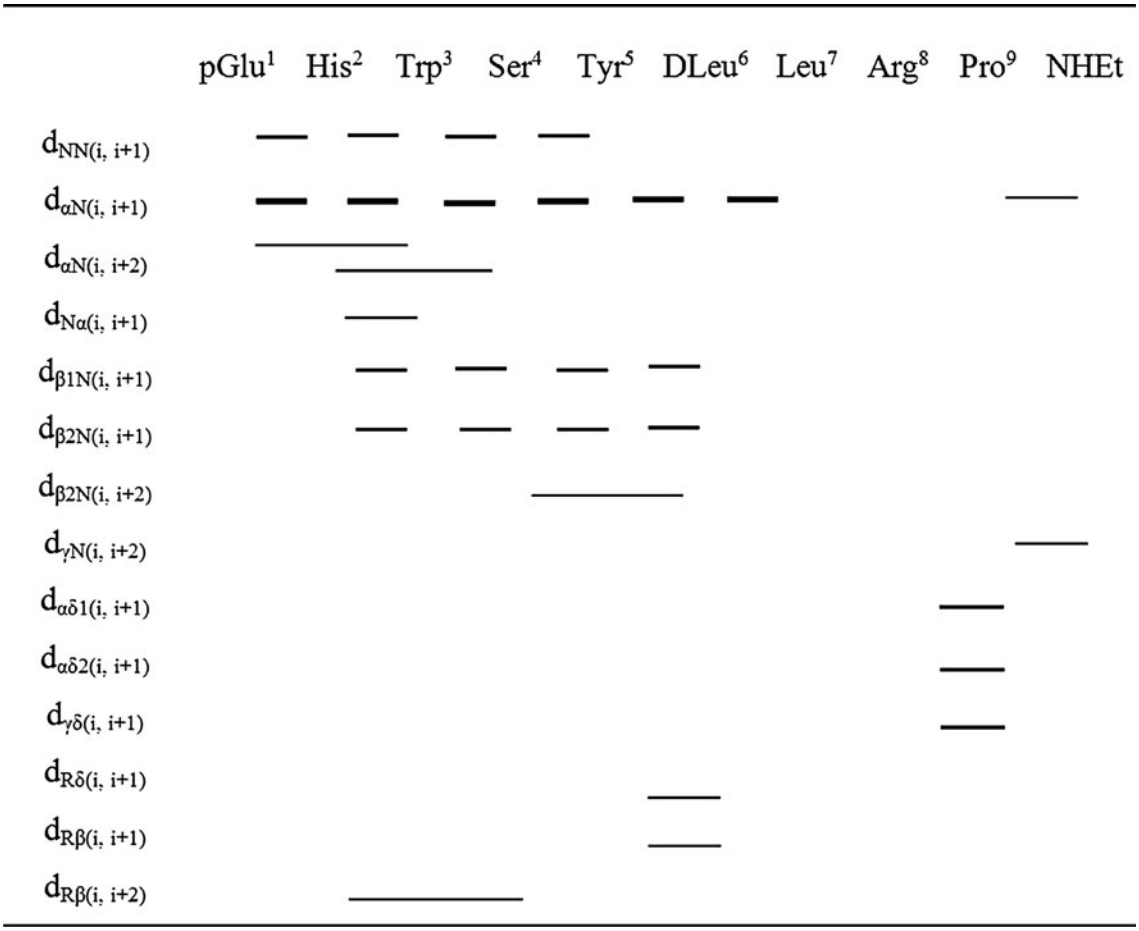

However, because there is a statistical variation associated with dihedral angles of ±30° (which is the error of calculated dihedral angles from NMR data), the type III β-turn is often classified under the type I β-turn category. The discrimination between type I and type III β-turn can be easily obtained by the $^3J_{HN,H\alpha}$ value of the coupling constant of residue 3 (Ser^4). In the type III β-turn the $^3J_{HN,H\alpha}$ value is ~4 Hz, while in the type I β-turn it is ~8 Hz. In our case, a value of 7.3 Hz was calculated, indicating that the conformation of the His^2-Trp^3-Ser^4-Tyr^5 segment is more likely a type I β-turn.

Similarly, examining the TOCSY and the NOESY spectra of the [Tyr(OMe)^5, DLeu^6, NHEt^{10}]GnRH (2) analogue, all the necessary cross-peaks which are consistent with the presence of a type I β-turn, are observed (Fig. S1). Thus, the data proves the existence of a small but observable population of a type I β-turn in the segment His^2-Trp^3-Ser^4-Tyr^5 of [Tyr(OMe)^5, DLeu^6, NHEt^{10}]GnRH (2) analogue.

In the case of Leuprolide, all the necessary NOE cross-peaks are present, except of the Trp^3 H$^{\alpha}$-Tyr^5 H^N cross-peak, which is not observed (Fig. S2). Instead, a very weak Trp^3 H$^{\beta}$-Tyr^5 H^N is observed. Thus, the NOE data is consistent with the presence of a small but observable population (less than in the two previous analogues, due to the lack of an observable Trp^3 H$^{\alpha}$-Tyr^5 H^N cross-peak) of a type I β-turn in the segment His^2-Trp^3-Ser^4-Tyr^5 of Leuprolide. Furthermore, a downfield transposition in the chemical shift of the NH$^{\varepsilon}$ of the guanidine group of Arg^8 was observed, indicating the participation of the NH$^{\varepsilon}$ proton in a hydrogen bond. Since this transposition was not observed in [Tyr(OMe)^5, DLeu^6, Aze^9, NHEt^{10}]GnRH (1) and [Tyr(OMe)^5, DLeu^6, NHEt^{10}]GnRH (2) analogues, where the hydrogen atom of the hydroxyl group of Tyr^5 has been substituted by a methyl group, we can assume that the hydrogen bond is formed between the guanidine group of Arg^8 and the hydroxyl group of Tyr^5.

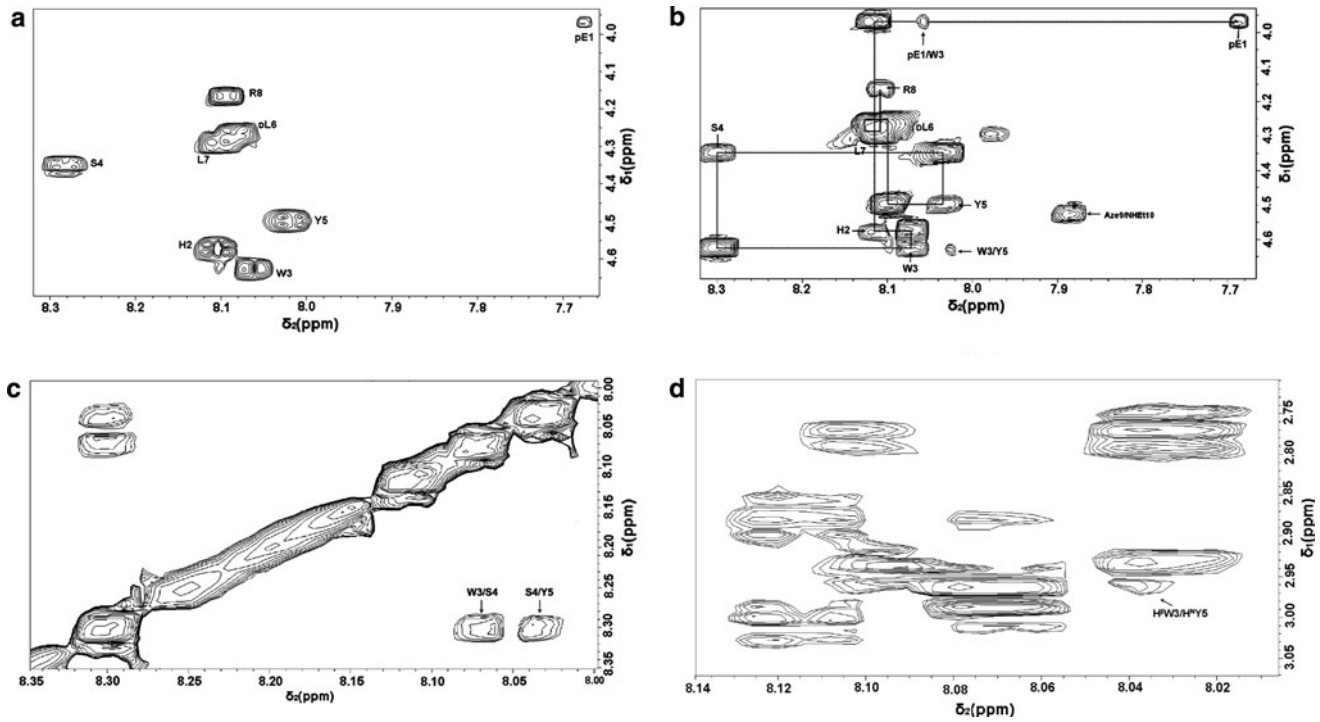

Fig. 1 NMR spectra of the linear analogue [Tyr(OMe)^5, DLeu^6, Aze^9, NHEt^{10}]GnRH (1) in DMSO. **a** The H$^{\alpha}$(δ_1)-H^{N}(δ_2) region of the TOCSY spectrum showing the backbone of the peptide. **b** The H$^{\alpha}$(δ_1)-H^{N}(δ_2) region of the NOESY spectrum. Sequential NOE connectivities corresponding to intra-residue H$^{\alpha}$(i)-H^{N}(i) and short range inter-residue H$^{\alpha}$(i)-H^{N}(i + 1) are shown, but only the intra-residue NOEs are labelled for simplicity. Weak cross-peaks correspond to the pGlu^1 H$^{\alpha}$-Trp^3 H^{N} and Trp^3 H$^{\alpha}$- Tyr(OMe)^5 H^{N} are shown. The last one is characteristic of a β-turn. **c** the H^{N}(δ_1)-H^{N}(δ_2) region of the NOESY spectrum. Cross-peaks corresponding to Trp^3 H^{N}- Ser^4 H^{N}, Ser^4 H^{N}-Tyr^5 H^{N}, NOEs are observed, which are characteristic of the presence of a type I β-turn. **d** H$^{\beta}$(δ_1)/H^{N}(δ_2) region of the NOESY spectrum. A very weak H$^{\beta}$(i)-H^{N}(i + 2) cross-peak is observed, corresponding to the Trp^3 H$^{\beta}$-Tyr^5 H^{N} NOE. This NOE is consistent with the presence of a small but observable population of a type I β-turn in the segment His^2-Trp^3-Ser^4-Tyr^5 of analogue 1

NMR characterisation of [DLeu^6, NHEt^{10}]GnRH (Leuprolide), [Tyr(OMe)^5, DLeu^6, Aze^9, NHEt^{10}]GnRH (1) and [Tyr(OMe)^5, DLeu^6, NHEt^{10}]GnRH (2) in H_2O-D_2O 90-10

Chemical shift overlaps in the H^{N} of Trp^3/Ser^4/DLeu^6/Leu^7 are present in the TOCSY spectrum of the [Tyr(OMe)^5, DLeu^6, Aze^9, NHEt^{10}]GnRH (1) analogue. Chemical shift overlaps in the H$^{\alpha}$ of DLeu^6/Arg^8 and partially of His^2/Trp^3 and Ser^4/Leu^7/Tyr^5 are present, too. These overlaps are a strong indication of the flexibility of this analogue. Sequential connectivities corresponding to intra-residue H$^{\alpha}$(i)-H^{N}(i) and short range H$^{\alpha}$(i)-H^{N}(i + 1) NOE cross-peaks are observed in Fig. 2a. In addition, a weak H$^{\alpha}$(i)-H^{N}(i + 2) cross-peak corresponding to Ser^4 H$^{\alpha}$-DLeu^6 H^{N} is observed, which is consistent with the presence of a β-turn. Figure 2b shows the H^{N} (δ_1)-H^{N} (δ_2) region of the NOESY spectrum of [Tyr(OMe)^5, DLeu^6, Aze^9, NHEt^{10}]GnRH (1) analogue, where the observed H^{N}(i)-H^{N}(i + 1) cross-peaks are labelled. Medium intensity cross-peak corresponding to Ser^4 H^{N}-Tyr^5 H^{N} and strong cross-peak corresponding to Tyr^5 H^{N}-DLeu^6 H^{N} NOEs are observed, which are consistent with the presence of a type II β-turn in the segment Trp^3-Ser^4-Tyr^5-DLeu^6. This is further confirmed by the existence of the strong intensity Ser^4 H$^{\alpha}$-Tyr^5 H^{N} cross-peak which is observed in Fig. 2a. The above NOE data is consistent with the presence of a small but observable population of a type II β-turn in the segment Trp^3-Ser^4-Tyr^5-DLeu^6 of [Tyr(OMe)^5, DLeu^6, Aze^9, NHEt^{10}]GnRH (1) analogue. The type II β-turn is further confirmed by the $^3J_{HN,H\alpha}$ value of the coupling constant of residue 3 (Tyr^5). In the type II β-turn the $^3J_{HN,H\alpha}$ value is $\sim$5 Hz, while in the type I β-turn it is $\sim$8 Hz. In our case, a value of 5.4 Hz was calculated, indicating that the conformation of the Trp^3-Ser^4-Tyr^5-DLeu^6 segment is more likely a type II β-turn. A very weak cross-peak corresponding to His^2 H^{N}-NHEt^{10} H^{N} is observed, indicating that a U-shape conformation of this analogue must be taken in consideration.

Figure S3a shows the H$^{\alpha}$ (δ_1)-H^{N} (δ_2) region of the NOESY spectrum of [Tyr(OMe)^5, DLeu^6, NHEt^{10}]GnRH (2) analogue. Sequential connectivities corresponding to intra-residue H$^{\alpha}$(i)-H^{N}(i) and short range H$^{\alpha}$(i)-H^{N}(i + 1) NOE cross-peaks are observed, but a weak H$^{\alpha}$(i)-H^{N}(i + 2)

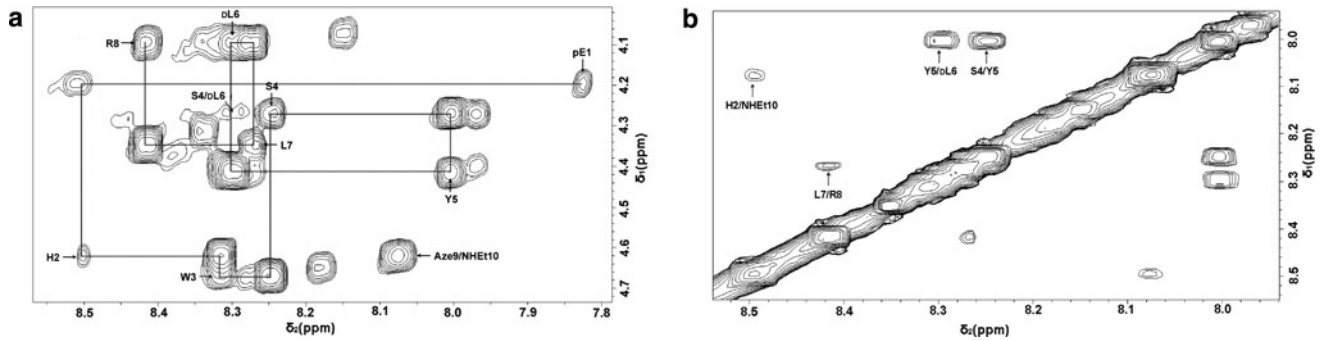

Fig. 2 NMR spectra of the linear analogue [Tyr(OMe)^5, DLeu^6, Aze^9, NHEt^{10}]GnRH (1) in H_2O D_2O 90–10. **a** The $H^{\alpha}(\delta_1)$-$H^N(\delta_2)$ region of the NOESY spectrum. Sequential NOE connectivities corresponding to intra-residue $H^{\alpha}(i)$-$H^N(i)$ and short range inter-residue $H^{\alpha}(i)$-$H^N(i + 1)$ are shown, but only the intra-residue NOEs are labelled for simplicity. Weak cross-peak corresponds to the Ser^4 H^{α}-DLeu^6 H^N is shown, characteristic of a β-turn. **b** The $H^N(\delta_1)$-$H^N(\delta_2)$ region of the NOESY spectrum. Cross-peaks corresponding to Ser^4 H^N-Tyr(OMe)^5 H^N, Tyr(OMe)^5H^N- DLeu^6 H^N, NOEs are observed, which are characteristic of the presence of a type II β-turn

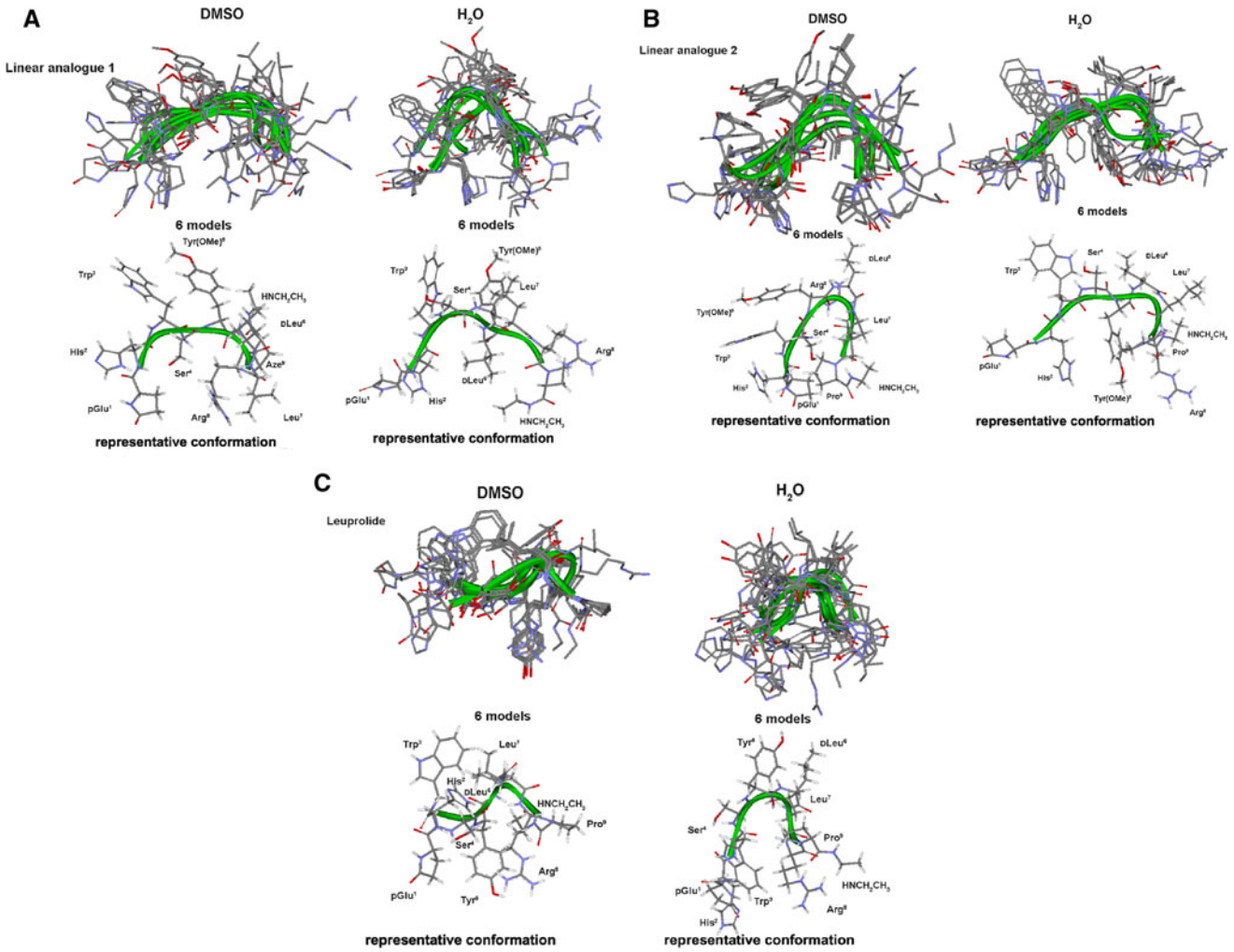

Fig. 3 **a** Family of 6 energy-minimised models calculated for linear analogue (**1**) [Tyr(OMe)^5, DLeu^6, Aze^9, NHEt^{10}]GnRH in DMSO and H_2O solutions and the most representative selected conformations respectively, **b** Family of 6 energy-minimised models calculated for linear analogue (**2**) [Tyr(OMe)^5, DLeu^6, NHEt^{10}]GnRH in DMSO and H_2O solutions and the most representative selected conformations respectively and **c** Family of 6 energy-minimised models calculated Leuprolide [DLeu^6, NHEt^{10}]GnRH in DMSO and H_2O solutions and the most representative selected conformations respectively

cross-peak corresponding to Ser^4 H^{α}-DLeu^6 H^N is not observed. Figure S3b shows the H^N (δ_1)-H^N (δ_2) region of the NOESY spectrum of [Tyr(OMe)^5, DLeu^6, NHEt^{10}]GnRH (2) analogue. Weak to medium intensity cross-peaks corresponding to Ser^4 H^N-Tyr^5 H^N and to Tyr^5 H^N-DLeu^6 H^N NOEs are observed. Also, a $^3J_{HN,H\alpha}$ value of 5.2 Hz was calculated for Ser^4. From the observed $H^N(i)$-$H^N(i+1)$ cross-peaks we can assume that [Tyr(OMe)^5, DLeu^6, NHEt^{10}]GnRH (2) analogue has a propensity to form a β-turn, but the data also suggests an increased flexibility or alternatively reduced population of the β-turn in [Tyr(OMe)^5, DLeu^6, NHEt^{10}]GnRH (2) analogue compared with [Tyr(OMe)^5, DLeu^6, Aze^9, NHEt^{10}]GnRH (1) analogue in water solution.

Sequential connectivities corresponding to intra-residue $H^{\alpha}(i)$-$H^N(i)$ and short range $H^{\alpha}(i)$-$H^N(i+1)$ NOE cross-peaks are observed in NOESY spectrum of Leuprolide (Fig. S4a). Figure S4b shows the H^N (δ_1)-H^N (δ_2) region of the NOESY spectrum of Leuprolide. A medium intensity cross-peak corresponding to DLeu^6 H^N-Leu^7 H^N and a weak intensity cross-peak corresponding to Tyr^5 H^N-DLeu^6 H^N NOEs are observed, which suggest the presence of a type II β-turn in the segment Ser^4-Tyr^5-DLeu^6-Leu^7. A weak $H^{\alpha}(i)$-$H^N(i+2)$ cross-peak corresponding to Tyr^5 H^{α}-Leu^7 H^N, which is necessary for the existence of a β-turn is not observed unambiguously, due to chemical shift overlapping of Tyr^5/Leu^7 in the H^{α} dimension (Fig. S4a). But, the presence of a type II β-turn in the segment Ser^4-Tyr^5-DLeu^6-Leu^7 is further confirmed by the existence of the strong intensity Tyr^5 H^{α}-DLeu^6 H^N cross-peak which is observed in Fig. S4a. The above NOE data denotes the possible presence of a small but observable population of a type II β-turn in the segment Ser^4-Tyr^5-DLeu^6-Leu^7 of Leuprolide.

Insight into the bioactive conformation of GnRH analogues

The MD simulation results a wide range of conformations of the studied GnRH analogues. Among the 500 energy minimised conformations that were obtained after 1 ns molecular dynamic simulation, the most representative conformations were selected examining their energy calculation (time vs. energy plots, data not shown), the energy convergence criterion root mean square deviation (RMSD force $\leq$0.001 kcal mol^{-1}Å^{-1}) and last but not least the results extracting form 2D H^1-H^1 TOCSY and NOESY spectrums. More specifically, the adopted conformations examined using the observed inter-residue cross-peaks in the NOESY spectrum and their intensities which can be translated as distances between hydrogens of the amino acids of the analogues. Moreover, dihedral angles [$\varphi_{(i+1)}$, $\psi_{(i+1)}$, $\varphi_{(i+2)}$, $\psi_{(i+2)}$] of the characteristic turns (results extracted from NMR experiments, see above the NMR characterisation) were used in order to identify the most representative conformations of the studied analogues.

Side chains present a slightly different topology as seen, but this is expected as it is known that flexible molecules can be deformed when binding to proteins (Nicklaus et al. 1995). Therefore, this methodology can be established as a robust method for identifying putative bioactive conformations, even when X-ray data are absent. Theoretical methods arise as a solution for exploration of conformational space in the vicinity of conformers deduced from spectroscopic data and offer starting conformations for the conformational studies at the receptor-binding site. Using the criteria described above (NMR and Molecular Dynamics results), the representative conformations for Leuprolide and its two linear analogues are indicated in Fig. 3.

Generally these conformations adopt a U-shape feature which is the main structure characteristic for GnRH agonistic analogues when approach and bind to receptor based on theoretical studies (Söderhäll et al. 2005). It is obvious that these selected structures could not be totally characterised as 'bioactive' as no crystallographic data for the active site of GnRH receptor is available in the literature. Another structural characteristic of the studied analogues is that the aromatic rings of His^2, Trp^3 and Tyr^5 are in close proximity only in DMSO while these side chains and the guanidine group of Arg^8 are exposed in the external side of the U-shape (solvent) so as to interact with GnRH receptor. From the above conformational analysis it is evident that the amino acids His^2, Trp^3 and Arg^8 have a different orientation depended on the solvent used especially in analogue **(1)** and **(2)**. To quantify the relative change of the position of the imidazole His^2, indole Trp^3 and guanidino Arg^8 groups, the angles and the sides of the triangle formed by the centroids of the groups were measured (Table 4; Fig. 4). This data indicates the internal distances between the most important for binding and activation to the GnRH receptor indole, imidazole and guanidine group (Millar

Table 4 Geometries of triangles formed by centroids of side chain group of His^2, Trp^3 and Arg^8, for the putative bioactive conformation of Leuprolide, Analogue **1** and **2**

	Analogue 1		Analogue 2		Leuprolide	
	DMSO	H_2O	DMSO	H_2O	DMSO	H_2O
d (cHis^2-cTrp^3)	7.88 Å	11.24 Å	4.41 Å	10.89 Å	7.80 Å	6.21 Å
d (cHis^2-cArg^8)	12.10 Å	15.30 Å	12.13 Å	11.31 Å	9.89 Å	9.43 Å
d (cTrp^3-cArg^8)	13.43 Å	15.85 Å	10.63 Å	18.17 Å	12.76 Å	12.03 Å
a (cHis^2-cTrp^3-cArg^8)	62.2°	66.6°	98.7°	38.6°	51.2°	51.3°
a (cTrp^3-cHis^2-cArg^8)	81.4°	71.1°	60.3°	108.0°	91.8°	98.9°
a (cHis^2-cArg^8-cTrp^3)	36.4°	42.3°	21.0°	33.4°	37.0°	29.8°

a the angle

c the centroid of side chain

d the side length

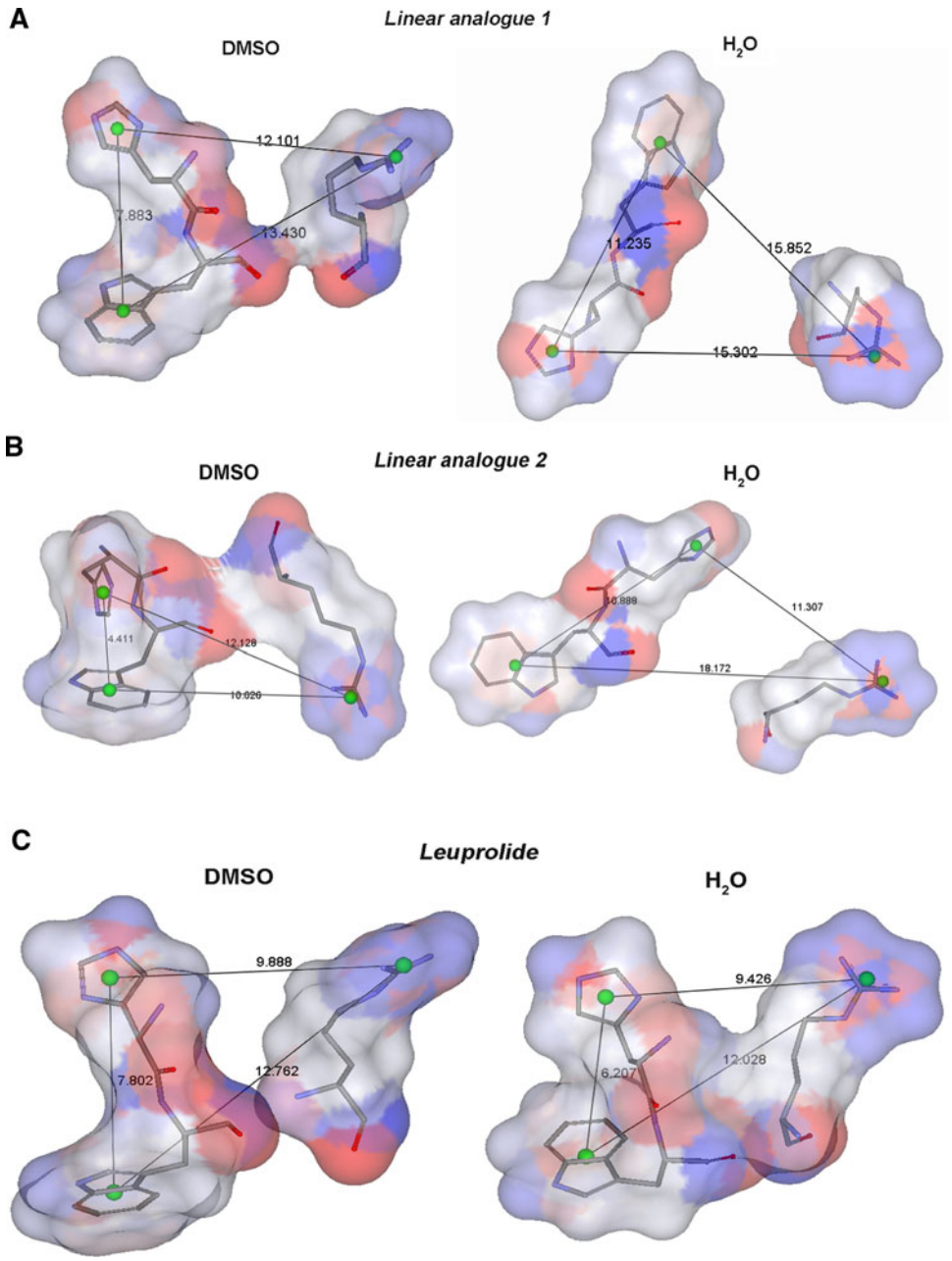

Fig. 4 Triangles formed by ring centroids of His[2], Trp[3] and Arg[8] for linear analogues **a** [Tyr(OMe)[5], DLeu[6], Aze[9], NHEt[10]]GnRH(**1**), **b** [Tyr(OMe)[5], DLeu[6], NHEt[10]]GnRH (**2**) and **c** Leuprolide in both DMSO and H_2O solutions. Length of the sides between the centroids is shown with *black lines*

et al. 1986, 1989; Millar and King 1983, 1988; Muske 1993; Coy et al. 1975; Vilchez-Martinez et al. 1975) which could be placed to a rigid organic template in order to design and synthesise non-peptide mimetics.

Effect of Leuprolide, [Tyr(OMe)[5], DLeu[6], Aze[9], NHEt[10]]GnRH (1) and [Tyr(OMe)[5], DLeu[6], NHEt[10]]GnRH (2) on human breast cancer cell line, MCF-7

MCF-7 cells were seeded in 96-well plates at a density of 2×10^3 cells per well. The following day the media was replaced with fresh media and cells were treated with 1×10^{-7} M to 1×10^{-9} M peptide analogues; Leuprolide (Sigma), [Tyr(OMe)[5], DLeu[6], Aze[9], NHEt[10]]GnRH and [Tyr(OMe)[5], DLeu[6], NHEt[10]]GnRH. The cells were grown in DMEM 5% FCS (DCC) without phenol red. Every 48 h the analogues were replaced with fresh media. On day 6, the effect of all analogues on MCF-7 cell growth were tested using [^{3}H]-thymidine assay. Podophylotoxin was used as an internal positive control (data not shown).

Leuprolide has previously been shown to inhibit MCF-7 cell proliferation (Sica et al. 1992). The ability of linear [Tyr(OMe)[5], DLeu[6], Aze[9], NHEt[10]]GnRH and [Tyr(OMe)[5], DLeu[6], NHEt[10]]GnRH analogues to inhibit cell proliferation of MCF-7 cells compared to Leuprolide was demonstrated

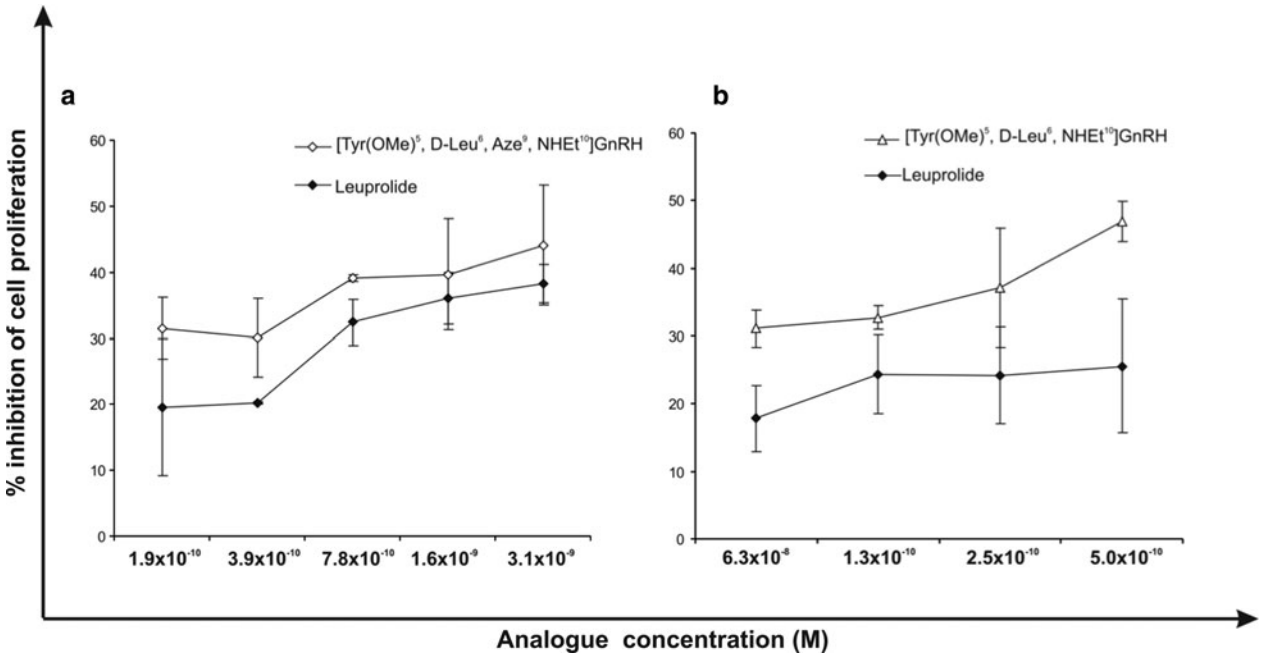

Fig. 5 Inhibition (% of cells alone) of estrogen-dependent human breast cancer cell line (MCF-7) proliferation using Leuprolide (*black diamond*) and **a** [Tyr(OMe)^5, DLeu^6, Aze^9, NHEt^{10}]GnRH (*white diamond*) or **b** [Tyr(OMe)^5, DLeu^6, NHEt^{10}]GnRH (*white triangle*), after 6 days. The results are mean ± standard error of mean (*SEM*) of triplicate wells. Representative result of five different experiments

(Fig. 5a, b). Linear [Tyr(OMe)^5, DLeu^6, Aze^9, NHEt^{10}] GnRH with changes at positions 5, 6, 9 was as effective in inhibiting cell proliferation compared to Leuprolide at concentrations of $<1 \times 10^{-9}$ M (Fig. 5a). At concentrations $<7.8 \times 10^{-10}$ M linear [Tyr(OMe)^5, DLeu^6, Aze^9, NHEt^{10}] GnRH was significantly better than Leuprolide. In addition, linear [Tyr(OMe)^5, DLeu^6, NHEt^{10}]GnRH with changes at the positions 5 and 6 was inhibitory to MCF-7 cell growth compared to Leuprolide at concentrations $<5 \times 10^{-7}$M (Fig. 5b). In particular, the anti-proliferative effect (% inhibition) was up to 44 and 46% for [Tyr(OMe)^5, DLeu^6, Aze^9, NHEt^{10}]GnRH and [Tyr(OMe)^5, DLeu^6, NHEt^{10}] GnRH, respectively (Fig. 5a, b).

In summary, the incorporation of [^{3}H]-thymidine into the DNA of MCF-7 cells was decreased by a 6 day treatment of cells with Leuprolide, linear [Tyr(OMe)^5, DLeu^6, Aze^9, NHEt^{10}]GnRH and linear [Tyr(OMe)^5, DLeu^6, NHEt^{10}] GnRH. Linear [Tyr(OMe)^5, DLeu^6, Aze^9, NHEt^{10}]GnRH is more efficient compared to linear [Tyr(OMe)^5, DLeu^6, NHEt^{10}]GnRH as it inhibits cell proliferation at lower concentrations $<1 \times 10^{-9}$M. Overall, substitution at the positions 5, 6 and 9 increases the inhibitory effect on MCF-7 cell proliferation at very low concentrations of GnRH analogues.

Conclusions

Molecular dynamics simulation in combination with NMR structure determination is used to search the conformational space for structures that fulfil the experimental distance restraints. The detailed NMR analysis has shown that Leuprolide, [Tyr(OMe)^5, DLeu^6, Aze^9, NHEt^{10}]GnRH (1) and [Tyr(OMe)^5, DLeu^6, NHEt^{10}]GnRH (2) analogues reveal almost similar structural characteristics. More specifically, in an aprotic-lipophilic solvent (DMSO), the most important finding is the existence a type I β-turn in the His^2-Trp^3-Ser^4-Tyr^5 segment in all analogues. Moreover, in Leuprolide, a downfield transposition in the chemical shift of the NH$^{\varepsilon}$ Arg^8 is observed, possibly due to the formation of a hydrogen bond between the guanidine group of Arg^8 and the hydroxyl group of Tyr^5 which in case of Leuprolide is not methylated. In a polar solvent (H_2O), a type II β-turn in the Trp^3-Ser^4-Tyr^5-DLeu^6 segment is observed in [Tyr(OMe)^5, DLeu^6, Aze^9, NHEt^{10}]GnRH (1), [Tyr(OMe)^5, DLeu^6, NHEt^{10}] GnRH (2) analogues, while in Leuprolide a type II β-turn is observed in the Ser^4-Tyr^5-Dleu^6-Leu^7 segment which agrees with previous published data (Meyer et al. 2002). The above observations indicate that the methyl group of Tyr and the mutation of Pro by Aze in synthesised analogues do not dramatically change the orientation of imidazole (His^2), indole (Trp^3) and guanidine (Arg^8) pharmacophore groups which are the most important for binding and activation of GnRH receptor. Moreover, the analogue [Tyr(OMe)^5, DLeu^6, Aze^9, NHEt^{10}]GnRH inhibits cell proliferation similarly or better to that of Leuprolide at very low concentrations where 30–40% inhibition is noted. The analogue [Tyr(OMe)^5, DLeu^6, NHEt^{10}]GnRH also inhibits cell proliferation in the range of 30–45% at low concentrations used.

At these concentrations it was clear that the synthesised analogues inhibit cell proliferation better than the control Leuprolide. At higher concentrations the difference in the inhibitory effect is not so clear, i.e. both analogues and control Leuprolide inhibit similarly. Thus, only small amounts of our analogues are required to see an inhibitory effect. In addition, the ability of methylated Tyr^5 and the use of Aze at position 9 to low the degree of desensitisation and increase stability of synthesised analogues make them useful in the future rational design of GnRH analogues.

Future work will include docking with the receptor followed by dynamics of the peptide-receptor complex, in order to obtain a refined preferable bioactive conformation that binds GnRH receptor. The knowledge of the relationship of peptide conformation and agonistic activity will lead to the rational design and synthesis of novel linear or cyclic peptide analogues and ultimately peptide mimetic molecules for the treatment of cancer.

Acknowledgments Despina Laimou is thankful for being supported by University of Patras (Grand K. Karatheodoris).

References

Discovery Studio v2.0 (2005), Molecular Modeling Systems, supplied by Accelrys Software Inc., Cerius^2 Modeling Environment, Release 4.8. Accelrys Software Inc, San Diego

Ayub M, Levell MJ (1990) Suppression of plasma androgens by the antiandrogen flutamide in prostatic cancer patients treated with Zoladex, a GnRH analogue. Clin Endocrinol 32:329–339

Brooks BR, Bruccoleri RE, Olafson BD, States DJ, Swaminathan S, Karplus M (1983) CHARMM: a program for macromolecular energy, minimization, and dynamics calculations. J Comp Chem 4:187–217

Chen J, Wonpil I, Brooks CL (2006) Balancing solvation and intramolecular interactions: toward a consistent generalized born force field. J Am Chem Soc 128(11):3373–3728

Conn PM, Crowley WF (1991) Gonadotropin-releasing hormone and its analogues. N Engl J Med 324(2):93–103

Coy DH, Coy EJ, Schally AV (1975) Research Methods in Neurochemistry. In: Marks N, Rodnight R (eds), Plenum, New York, pp 393–404

Hazum E, Conn PM (1988) Molecular mechanism of gonadotropin releasing hormone (GnRH) action, I: the GnRH receptor. Endocr Rev 9:379–386

Kaufmann M, Jonat W, Kleeberg U, Eiermann W, Janicke F, Hilfrich J, Kreienberg R, Albrecht M, Weitzel HK, Schmid H, Strunz P, Schachner-Wunschmann E, Bastert G, Maass H (1989) Goserelin, a depot gonadotropin-releasing hormone agonist in the treatment of pre-menopausal patients with metastatic breast cancer. J Clin Oncol 7:1113–1119

Keramida M, Matsoukas J, Panagiotopoulos D, Alexopoulos K, Matsoukas E, Cladas J, Tzigounis V, Cardamakis E, Maia H, Pati D, Habibi H (1996) Design and synthesis of a gonadotropin-releasing hormone (GnRH) analogue, [Tyr(OMe)5, D-Glu6, Aze9]GnRH: receptor binding, gonadotropin release and ovulation studies. Lett Pept Sci 3:257

Keramida M, Tselios T, Mantzourani E, Papazisis K, Mavromoustakos T, Klaussen C, Agelis G, Deraos S, Friligou I, Habibi H, Matsoukas J (2006). Design, synthesis, and molecular modeling of a novel amide-linked cyclic GnRH analogue cyclo(4-9)[Lys^4,D-Trp^6,Glu^9]GnRH: stimulation of gonadotropin gene expression. J Med Chem 49(1):105–110

Laskowski R, McArtur M, Moss D, Thornton J (1993) PROCHECK: a program to check the stereochemical quality of protein structures. J Appl Cryst 26:283–291

Mantzourani ED, Tselios TV, Golič Grdadolnik S, Platts JA, Brancale A, Deraos G, Matsoukas JM, Mavromoustakos TM (2006) Comparison of proposed putative active conformations of myelin basic protein epitope 87–99 linear altered peptide ligands by spectroscopic and modelling studies: the role of positions 91 and 96 in T-cell receptor activation. J Med Chem 49:6683–6691

Mantzourani ED, Platts JA, Brancale A, Mavromoustakos TM, Tselios TV (2007) Molecular dynamics at the receptor level of immunodominant myelin basic protein epitope 87–99 implicated in multiple sclerosis and its antagonists altered peptide ligands: triggering of immune response. J Mol Graph Model 26:471–481

Mantzourani ED, Blokar K, Tselios TV, Matsoukas JM, Platts JA, Mavromoustakos TM, Grdadolnik SG (2008) A combined NMR and molecular dynamics simulation study to determine the conformational properties of agonists and antagonists against experimental autoimmune encephalomyelitis. Bioorg Med Chem 16:2171–2182

Matsoukas J, Keramida M, Panagiotopoulos D, Mavromoustakos T, Maia HLS, Bigam G, Pati D, Habibi HR, Moore GJ (1997) Structure elucidation and conformational analysis of gonadotropin releasing hormone and its novel synthetic analogue [$Tyr(OMe)^5$, D-Lys^6, Aze^9NHEt]GnRH: the importance of aromatic clustering in the receptor binding activity. Eur J Med Chem 32:927–940

Matsoukas J, Apostolopoulos V, Kalbacher H, Papini AM, Tselios T, Chatzantoni K, Biagioli T, Lolli F, Deraos S, Papathanassopoulos P, Troganis A, Mantzourani E, Mavromoustakos T, Mouzaki A (2005) Design and synthesis of a novel potent myelin basic protein epitope 87–99 cyclic analogue: enhanced stability and biological properties of mimics render them a potentially new class of immunomodulators. J Med Chem 48:1470–1480

Meyer JD, Manning MC, Vander DG (2002) Velde, characterization of the solution conformations of leuprolide acetate. J Peptide Res 60:159–168

Millar RP, King JA (1983) Synthesis, luteinizing hormone-releasing activity, and receptor binding of chicken hypothalamic luteinizing hormone-releasing hormone. Endocrinology 113:1364–1369

Millar RP, King JA (1988) Evolution of gonadotropin-releasing hormone: multiple usage of a peptide. N Physiol Sci 3:49–53

Millar RP, Milton RC, Follett BK, King JA (1986) Receptor binding and gonadotropin-releasing activity of a novel chicken gonadotropin-releasing hormone ([His^5, Trp^7, Tyr^8]GnRH) and a D-Arg^6 analogue. Endocrinology 119:224–231

Millar RP, Flanagan CA, Milton RC, King JA (1989) Chimeric analogues of vertebrate gonadotropin-releasing hormones comprising substitutions of the variant amino acids in positions 5, 7, and 8 Characterization of requirements for receptor binding and gonadotropin release in mammalian and avian pituitary gonadotropes. J Biol Chem 264:21007–21013

Momany FA (1976) Conformational energy analysis of the molecule, luteinizing hormone-releasing hormone, 2: tetrapeptide and decapeptide analogues. J Am Chem Soc 98:2990–3000

Momany FA (1978) Conformational analysis of the molecule luteinizing hormone-releasing hormone, 3: Analogue inhibitors and antagonists. J Med Chem 21:63–68

Morikis D, Roy M, Sahu A, Troganis A, Jennings PA, Tsokos GC, Lambris JD (2002) The structural basis of compstatin activity

examined by structure-function-based design of peptide analogs and NMR. J Biol Chem 277:14942–14953

Muske LE (1993) Evolution of gonadotropin-releasing hormone (GnRH) neuronal systems. Brain Behav Evol 42:215–230

Nicklaus MC, Wang S, Driscoll JS, Milne GW (1995) Conformational changes of small molecules binding to proteins. Bioorg Med Chem 3:411

Ramachandran GN, Sasisekharan V (1968) Conformations of polypeptides and proteins. Adv Protein Chem 23:283–437

Ramakrishhan C, Ramachandran GN (1965) Stereochemical criteria for polypeptide and protein chain conformations, II: allowed conformations for a pair of peptide units. Biophys J 5:909–933

Ryckaert JP, Ciccotti G, Berendsen HJC (1977) Numerical integration of the cartesian equations of motion of a system with constraints: molecular dynamics of *n*-alkanes. J Comput Phys 23:327–341

Scambia G, Panici PB, Baiocchi G, Perrone L, Gaggini C, Iacobelli S, Mancuso S (1988) Growth inhibitory effect of LH-RH analogs on human breast cancer cells. Anticancer Res 8:187–190

Sica G, Iacopino F, Marini L, Robustelli della Cuna G (1992) Antiproliferative effect of leuprorelin acetate, alone or combined with tamoxifen or medroxyprogesterone acetate, on human breast cancer cell lines. Clin Ther 14:87–96

Söderhäll JA, Polymeropoulos EE, Pqulini K, Gunther E, Kuhne R (2005) Antagonist and agonist binding models of the human gonadotropin-releasing hormone receptor. Biochem Biophys Res Commun 333:568–582

Stephenson SL, Kenny AJ (1988) The metabolism of neuropeptides: hydrolysis of peptides by the phosphoramidon-insensitive rat kidney enzyme endopeptidase 2 and by rat microvillar membranes. Biochem J 255:45–51

Tselios T, Daliani I, Probert L, Deraos S, Matsoukas E, Roy S, Pires J, Moore G, Matsoukas J (2000a) Treatment of experimental allergic encephalomyelitis (EAE) induced by guinea pig myelin basic protein epitope 72–85 with a human MBP(87–99) analogue and effects of cyclic peptides. Bioorg Med Chem 8:1903–1909

Tselios T, Daliani I, Deraos S, Thymianou S, Matsoukas E, Troganis A, Gerothanassis I, Mouzaki A, Mavromoustakos T, Probert L, Matsoukas J (2000b) Treatment of experimental allergic encephalomyelitis (EAE) by a rationally designed cyclic analogue of myelin basic protein (MBP) epitope 72–85. Bioorg Med Chem Lett 10:2713–2717

Vignon F, Bouton MM, Rochefort H (1987) Antiestrogens inhibit the mitogenic effect of growth factors on breast cancer cells in the total absence of estrogens. Biochem Biophys Res Commun 146(3):1502–1508

Vilchez-Martinez LA, Coy DH, Coy EJ, Schally AV, Arimura A (1975) Anti-luteinizing hormone (LH)-releasing activity of several analogues of LH-releasing hormone. Fertil Steril 26:554–559

Wuthrich R (1986) NMR of proteins and nucleic acids. Wiley, New York